

Realizing bright matter-wave soliton collisions with controlled relative phase

T. P. Billam,* S. L. Cornish, and S. A. Gardiner

Department of Physics, Durham University, Durham DH1 3LE, United Kingdom

(Dated: November 19, 2021)

We propose a method to split the ground state of an attractively interacting atomic Bose-Einstein condensate into two bright solitary waves with controlled relative phase and velocity. We analyze the stability of these waves against their subsequent re-collisions at the center of a cylindrically symmetric, prolate harmonic trap as a function of relative phase, velocity, and trap anisotropy. We show that the collisional stability is strongly dependent on relative phase at low velocity, and we identify previously unobserved oscillations in the collisional stability as a function of the trap anisotropy. An experimental implementation of our method would determine the validity of the mean field description of bright solitary waves, and could prove an important step towards atom interferometry experiments involving bright solitary waves.

PACS numbers: 03.75.Lm, 05.45.Yv, 37.25.+k

Bright solitary waves (BSWs) in attractively-interacting atomic Bose-Einstein condensates (BECs) are an intriguing example of a nonlinear wave phenomenon in a degenerate quantum gas [1–3]. In the mean-field, Gross-Pitaevskii equation (GPE) description, BSWs in a quasi-1D BEC with no external (axial) trapping potential correspond exactly to bright solitons in the focusing nonlinear Schrödinger equation (NLSE)

$$i\frac{\partial\psi(x,t)}{\partial t} = \left[-\frac{1}{2}\frac{\partial^2}{\partial x^2} - |\psi(x,t)|^2 \right] \psi(x,t). \quad (1)$$

This integrable equation describes a diverse range of physical systems in addition to BECs [4], and its bright soliton solutions have been extensively studied in the context of nonlinear optics [5–9]. The addition of a harmonic trapping potential to Eq. (1) leads to non-integrability, but BSWs in harmonically trapped, quasi-1D BECs remain, in the GPE description, highly soliton-like; they collide elastically over a large parameter regime, and their asymptotic trajectories follow particle models applicable to solitons [10, 11]. Relaxing the quasi-1D restriction reduces the soliton character of BSWs further, but BSWs in the 3D GPE description retain many soliton-like characteristics [12], including an absence of dispersion and the existence of a *well-defined relative phase between BSWs*. If actual 3D BSWs possess a well-defined relative phase when realized experimentally, one can envisage a BSW interferometer, akin to current matter-wave interferometers but leveraging the small size, coherence, and non-dispersive nature of BSWs [2]. Indeed, BSWs have already been proposed as a metrological tool for the study of atom-surface interactions [13].

Experiments to date have produced both individual [1] and multiple [2, 3] BSWs as remnants from the collapse [14, 15] of a larger condensate. These BSWs were capable, in the case of multiple BSWs, of surviving many mutual re-collisions at the trap center [2, 3]. In the quasi-1D regime the observed BSW motion matches the GPE description of BSWs with relative phase $\Phi = \pi$ [2, 16]. In the 3D regime, however, BSWs are not universally stable against multiple re-collisions; numerical integration of the GPE reveals that slow 3D BSWs retain their form for fewer collisions when their relative phase, Φ ,

is equal to 0 than when $\Phi = \pi$ [12]. The long lifetimes of 3D BSWs seen in experiment thus seem to imply that their relative phase $\Phi = \pi$ [3, 12]. Modulational instability and the shorter lifetime of colliding 3D BSWs when $\Phi = 0$ have been identified as contributory causes to these apparent anti-phase relations in both regimes [12, 16, 17]. However, recent simulations of BSW collisions incorporating quantum noise have been interpreted as showing the dynamics and collisional stability of BSWs to be *phase-independent*, with the dynamics for *all* relative phases corresponding to the GPE description for $\Phi = \pi$ [18]. Furthermore, no 3D GPE simulation of the collapse process has produced BSW remnants matching those observed in experiment [18]. These considerations leave the question open: *are experimentally observed atomic BSWs well-described by an effective single-particle wavefunction, propagated by the GPE?*

In this letter we propose an experiment to answer this question. We describe a method which, in a velocity- and phase-controlled way, splits a single BSW in an axisymmetric harmonic trap into two outgoing BSWs which repeatedly re-collide at the trap center. Using the GPE, we demonstrate that such pairs of BSWs can be realized in an atomic BEC, and analyze their dynamics and collisional stability. We explore the crossover from quasi-1D to fully 3D regimes, examining the effects of velocity and relative phase on the number of collisions for which the BSWs remain soliton-like, C_{1D} . In addition to demonstrating the expected C_{1D} phase dependence for slow collisions, we show that C_{1D} has a strong oscillatory dependence on the trap anisotropy, due to resonances between the frequency of the BSWs' radial oscillations and the frequency with which the two BSWs collide. The experimental presence (absence) of the predicted phase and anisotropy dependencies would indicate the (in)sufficiency of the GPE description of BSWs; either of these outcomes would be an important result. In particular, sufficiency of the GPE description implies a well-defined relative phase between BSWs, paving the way for future atom interferometry experiments using BSWs, towards which our proposed BSW generation method would represent an important step.

We begin with the GPE for a BEC of N atoms of mass m

and (attractive) s -wave scattering length $a_s < 0$, held within a cylindrically symmetric, prolate harmonic trap,

$$i\hbar \frac{\partial \Psi(\mathbf{r}, t)}{\partial t} = \left[-\frac{\hbar^2}{2m} \nabla^2 + V(\mathbf{r}) - |g_{3D}| |\Psi(\mathbf{r}, t)|^2 \right] \Psi(\mathbf{r}, t), \quad (2)$$

where $g_{3D} = 4\pi N a_s \hbar^2 / m$, the condensate wavefunction $\Psi(\mathbf{r}, t)$ is normalized to one, and $V(\mathbf{r}) = m[\omega_x^2 x^2 + \omega_r^2 (y^2 + z^2)]/2$, where ω_x and $\omega_r > \omega_x$ are the axial and radial trap frequencies. With strong radial confinement the system is quasi-1D and can be described by Eq. (2) with $\Psi(\mathbf{r}, t) \rightarrow \Psi(x, t)$, $V(\mathbf{r}) \rightarrow m\omega_x^2 x^2/2$, and $g_{3D} \rightarrow g_{1D} = 2\hbar\omega_r |a_s| N$ [19]. The resulting configuration has two key length scales; the harmonic length $a_0 = \sqrt{\hbar/m\omega_x}$, and the soliton length $b_0 = \hbar^2/mg_{1D}$. Rescaling all lengths to units of b_0 and all times to units of \hbar^3/mg_{1D}^2 [10] produces the dimensionless 1D GPE

$$i \frac{\partial \psi(x, t)}{\partial t} = \left[-\frac{1}{2} \frac{\partial^2}{\partial x^2} + \frac{\omega^2 x^2}{2} - |\psi(x, t)|^2 \right] \psi(x, t), \quad (3)$$

where $\omega = (b_0/a_0)^2$ is a dimensionless effective trap strength [20]. In this letter, we consider the effects of abruptly increasing the scattering length magnitude in such a BEC from initial a_s^0 to $a_s = \alpha^2 a_s^0$ ($\alpha > 1$ and $a_s, a_s^0 < 0$), with initial condition

$$\psi(x, t = 0) = \psi_0(x) = \psi_\alpha(x) \cos\left(\frac{kx}{2\alpha^2} + \frac{\Phi}{2}\right), \quad (4)$$

where $\psi_\alpha(x)$ is the BSW ground state of the BEC for scattering length a_s^0 . We first consider the quasi-1D limit, where a stable ground state $\psi_\alpha(x)$ always exists, and then 3D, where the stable ground state $\psi_\alpha(\mathbf{r})$ exists only for $|a_s^0|$ below the critical value for the onset of collapse, $|a_s^c|$ [15].

The ground state $\psi_\alpha(x)$ may be made by using a magnetic Feshbach resonance to adiabatically change the scattering length from being initially repulsive to a negative value, a_s^0 , with $|a_s^0| < |a_s^c|$. The rapid change from a_s^0 to $a_s = \alpha^2 a_s^0$ could then exploit the same resonance. The density modulation that transforms $\psi_\alpha(x)$ into $\psi_0(x)$ may be achieved with a second internal atomic state in an interference protocol: writing the total state of the condensed atoms as $\psi_+(x)|+\rangle + \psi_-(x)|-\rangle$, we begin with all atoms in internal state $|+\rangle$ [i.e., $\psi_+(x) = \psi_\alpha(x)$ and $\psi_-(x) = 0$]. Applying a resonant $\pi/2$ pulse to the internal state transition yields $\psi_+(x) = \psi_-(x) = \psi_\alpha(x)/\sqrt{2}$. We now imprint equal and opposite momenta on the two internal states, giving $\psi_\pm(x) = \exp[\pm i(Kx + \Phi)/2] \psi_\alpha(x)/\sqrt{2}$, which is then transformed into

$$\begin{aligned} \psi_+(x) &= \cos[(Kx + \Phi)/2] \psi_\alpha(x), \\ \psi_-(x) &= i \sin[(Kx + \Phi)/2] \psi_\alpha(x), \end{aligned} \quad (5)$$

by a second $\pi/2$ pulse. Using resonant light to rapidly expel atoms in state $|-\rangle$ from the trap leaves those in state $|+\rangle$ with wavefunction $\psi_0(x)$ [Eq. (4)], with $k = \alpha^2 K$, and with Φ determined by the phase accumulated at the center of the BSW. Note that the loss of atoms between $\psi_\alpha(x)$ and $\psi_0(x)$ is balanced by the change in normalization; N denotes the *initial* atom number. There are many potential implementations

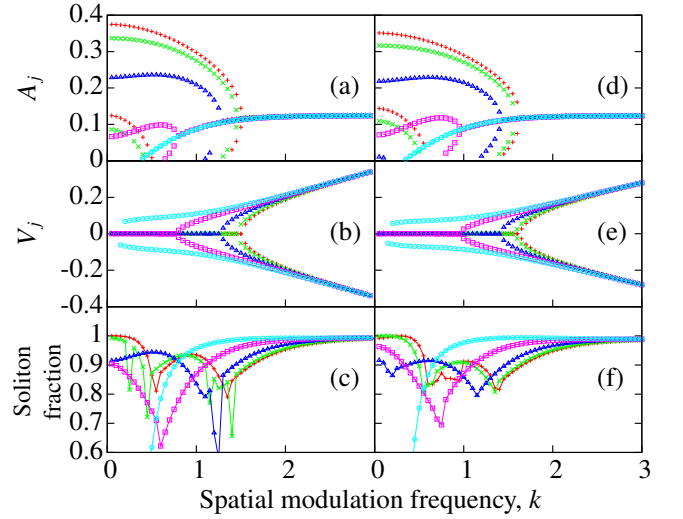


FIG. 1. (color online). The structure of a multi-soliton pulse. The panels show the soliton amplitudes A_j , velocities V_j , and fractions associated with the initial condition $\psi_0(x)$ [Eq. (6)] in the NLSE [Eq. (1)], computed using a numerical scattering transform [24], as a function of spatial modulation frequency k . Panels (a–c) correspond to $\alpha = 2$ and (d–f) to $\alpha = 2.2$. Relative phases are $\Phi = 0$ (+), $\pi/4$ (x), $\pi/2$ (Δ), $3\pi/4$ (\square), π (\circ). Soliton fraction is the ratio of the combined norm of the constituent solitons, $\sum_j 2A_j$, to the total norm $\int_{-\infty}^{\infty} |\psi_0(x)|^2 dx$ [23]. In the limit $k \rightarrow \infty$, when $\alpha = 2$, $A_j \rightarrow 1/8$ [$\sum_j 2A_j \rightarrow \int_{-\infty}^{\infty} |\psi_0(x)|^2 dx \rightarrow 1/2$], and $V_j \rightarrow \pm k/8$ [8, 9].

of this protocol. Using a two-component GPE, we have simulated an implementation that uses ^{85}Rb atoms in the quasi-1D regime with an applied magnetic field gradient to transfer momentum: we find this simple prototype to be capable of generating initial conditions close to Eq. (4) using current experimental technology [21].

Neglecting the axial trapping (setting $\omega = 0$) the 1D GPE [Eq. (3)] reduces to the NLSE [Eq. (1)], and the ground state of the BEC before the change in scattering length, $\psi_\alpha(x)$, is a single, stationary bright soliton [23]. After density modulation

$$\psi_0(x) = \frac{1}{2\alpha} \operatorname{sech}\left(\frac{x}{2\alpha^2}\right) \cos\left(\frac{kx}{2\alpha^2} + \frac{\Phi}{2}\right). \quad (6)$$

Solutions of the NLSE for this initial condition [Eq. (6)] are well-known in the context of nonlinear optics [7–9]. The case $k = 0$ has been studied analytically by Satsuma and Yajima [7] using the inverse scattering transform (IST) [5]: for integer $\alpha = J$, Eq. (6) consists of a bound state, or multi-soliton pulse, of J solitons with unequal amplitudes A_j and zero velocity ($V_j = 0$). For non-integer $\alpha = J + \beta$, Eq. (6) consists of J solitons plus scattered radiation, with the norm of the soliton component given by $\sum_j 2A_j$ [7, 23]. The modulated case (general k) has been considered both analytically and numerically by Kodama and Hasegawa [8] and Afanasjev and Vysloukh [9]. Fig. 1 shows how the modulation alters the character of a two soliton pulse ($\alpha \gtrsim 2$): beyond a certain threshold value of k the

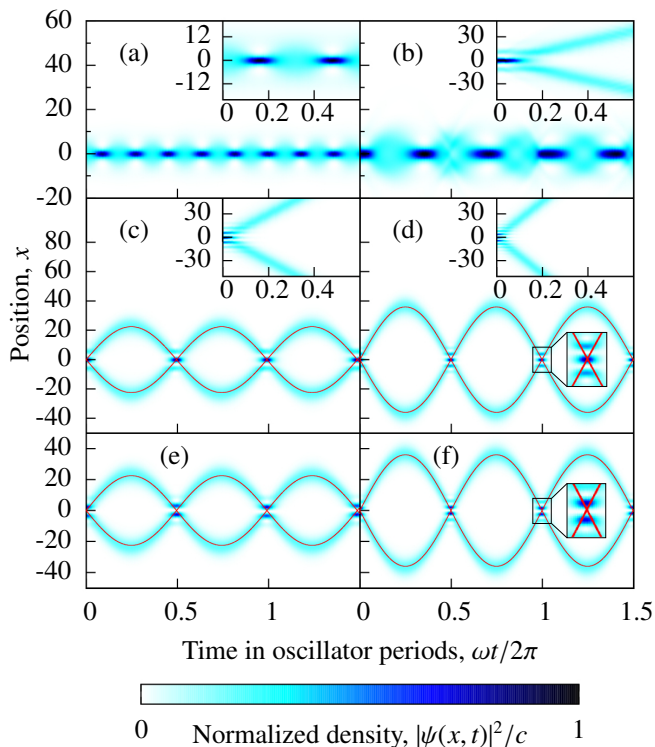


FIG. 2. (color online). Generation of BSWs with controlled relative phase via the interference protocol, in the quasi-1D limit. Panels (a–f) show the evolution of 1D GPE with trap frequency $\omega = 0.02$ [$\omega = 0$ inset in (a–d)] and initial condition $\psi_0(x)$ for $\alpha = 2$, $\Phi = 0$ and $k = 0$ (a), $k = 2$ (b), $k = 4$ (c), $k = 6$ (d), and $\Phi = \pi$ and $k = 4$ (e), $k = 6$ (f), computed using a pseudospectral split-step method. Particle model [10] BSW trajectories, for effective masses and velocities obtained from the numerical scattering transform of $\psi_0(x)$, are overlaid as lines in (c–f). Panels (e) and (f) reproduce (c) and (d) for the case $\Phi = \pi$ to show the difference in collision profile. The density (color) axes are normalized by $c = 0.35$ (inset $c = 0.25$) in (a) and $c = 0.12$ (inset $c = 0.07$) in (b–f).

pulse “splits” into two solitons with equal amplitudes, opposite velocities, and relative phase Φ , plus a negligible radiation component. Crucially, control of the modulation corresponds to control over the relative velocity and phase of a pair of generated bright solitons.

A similar correspondence exists in the presence of axial trapping ($\omega > 0$). In this regime the 1D GPE [Eq. (3)] has no soliton solutions so we study the dynamics of initial condition $\psi_0(x)$ numerically, concentrating, for simplicity, on the case $\alpha = 2$ (other cases $\alpha \geq 2$ are similar except for a slightly altered relationship between k and the resulting soliton speed). A pair of equal amplitude BSWs are generated with relative phase Φ and velocities controlled by k [Fig. 2]. The axial trap confines the outgoing BSWs and causes subsequent recollisions at the trap center, and the relative phase upon recollision is always identical to the original imposed relative phase [10]. The BSWs remain highly soliton-like: the density profile during BSW collisions is similar to that for bright

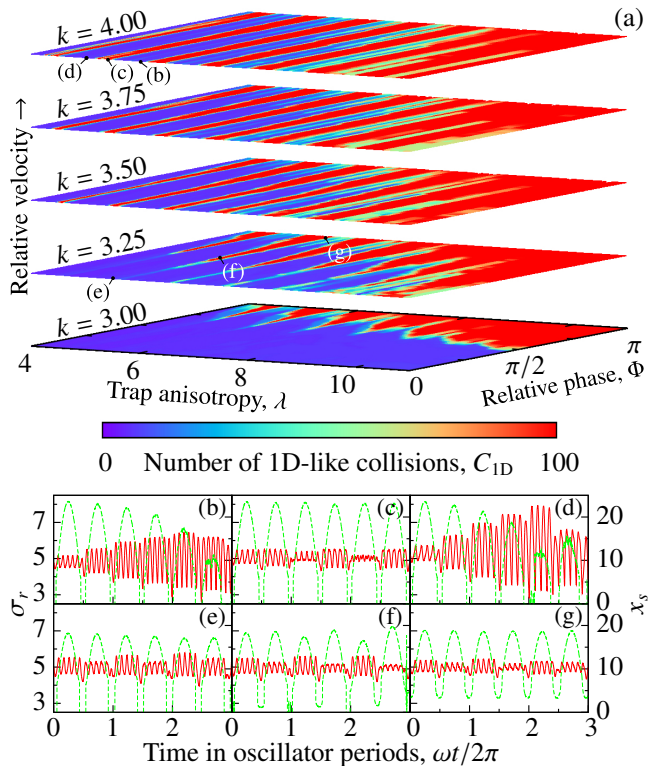


FIG. 3. (color online). Stability of BSW collisions in 3D. Panel (a) shows the number of 1D-like BSW collisions, C_{1D} , as a function of k , Φ , and λ [26]. Effective trap frequency $\omega = 0.02$ and $\alpha = 2$. Also shown is the evolution of the positively displaced BSW position, x_s (dashed green line, right vertical axis), and the full width at half maximum of the integrated radial density distribution, σ_r (solid red line, left vertical axis), at the indicated points on the $k = 4$ (b–d) and $k = 3.25$ planes in (a). The computation leverages the radial symmetry of the problem, using a pseudospectral split-step method in 2D cylindrical coordinates.

solitons [6] [Fig. 2(d,f)], the BSW trajectories are well described by a particle model [10, 11] [Fig. 2(c–f)], and the BSWs are stable against their mutual collisions, insofar as they retain their form for a sufficiently large number of collisions that atom losses, unaccounted for in the GPE, would be the lifetime-limiting factor in an experiment.

Moving beyond the quasi-1D regime, we can generate pairs of 3D BSWs with controlled velocity and relative phase using the same method. Dynamics in the radial directions can affect the stability of the BSWs, however; in certain cases this drastically reduces the number of collisions for which they retain their form. Parameterizing the quasi-1D-to-3D transition by the trap anisotropy $\lambda = \omega_r/\omega_x$, we write the 3D GPE as

$$i \frac{\partial \psi(\mathbf{r}, t)}{\partial t} = \left[-\frac{\nabla^2}{2} + V(\mathbf{r}) - \frac{2\pi}{\lambda\omega} |\psi(\mathbf{r}, t)|^2 \right] \psi(\mathbf{r}, t), \quad (7)$$

where we use soliton variables [25], and $V(\mathbf{r}) = \omega^2[x^2 + \lambda^2(y^2 + z^2)]/2$. We again study the dynamics of the BSWs numerically, quantifying their stability against collisions in

terms of their positions and maximum integrated axial densities at the point of maximum separation — this being much easier to measure, on typical experimental scales, than the exact density profile during the collision. Fig. 3(a) shows how the number of 1D-like collisions C_{1D} (taken to be those where the positions and maximum integrated densities of the BSWs subsequently return to within 75% of their original values) depends on velocity, relative phase, and trap anisotropy. We term these collisions 1D-like because all collisions of quasi-1D BSWs satisfy these criteria ($C_{1D} \rightarrow \infty$).

As expected, Fig. 3(a) shows that C_{1D} is strongly dependent on the relative phase at low velocity, with the BSWs being most stable around $\Phi = \pi$ outside the quasi-1D regime [26]. At higher velocity this phase-dependence weakens and the quasi-1D regime is reached at lower anisotropy. Fig. 3(a) also reveals a previously unobserved feature: C_{1D} shows a strong, oscillatory dependence on the anisotropy at all velocities. This dependence arises from the BSWs being broken up by the transfer of energy to radial oscillations [Fig. 3(b–d)]. These oscillations are started by the abrupt change in scattering length, and subsequently amplified by collisions if the BSWs collide when their radial width is close to its oscillatory maximum. The frequency of the radial oscillations is primarily determined by ω_r ; this leads to the observed oscillations of C_{1D} as a function of λ . The amplifying effect of collisions decreases with the BSW velocity, and at low velocity a phase-dependent amplification of the radial oscillations emerges [Fig. 3(e–g)], which we attribute to the higher densities at the point of collision when $\Phi = 0$ delivering a larger “kick” than when $\Phi = \pi$. However, for intermediate phases symmetry-breaking population transfer [12, 27] during collisions also contributes to the reduction in C_{1D} [Fig. 3(f)]. Within the GPE description, Fig. 3 represents a comprehensive prediction of the BSW dynamics resulting from our splitting protocol. Experimental observation of the dynamics we predict would support the validity of the GPE description of BSWs and, in the case of the oscillatory dependence of C_{1D} on λ , open the possibility of controlling the BSW lifetime directly.

To conclude, we have proposed an experiment that produces a pair of BSWs with controlled relative phase and velocity in a harmonically trapped atomic BEC, and we have analyzed the subsequent collisions of these BSWs using the GPE. In the quasi-1D regime the BSWs are highly soliton-like and stable against their re-collisions. In the fully 3D regime, we confirm that the collisional stability of the BSWs depends on their relative phase and velocity, and demonstrate for the first time a strong oscillatory dependence on the trap anisotropy. The presence, or absence, of these effects in experiments provides a direct test of whether experimentally observed atomic BSWs can be described in terms of a coherent effective single-particle wavefunction, propagated by the GPE.

We thank N. G. Parker, S. A. Wrathmall, and P. M. Sutcliffe for many stimulating discussions, and UK EPSRC (Grant No. EP/G056781/1), the Royal Society (SLC), and Durham University (TPB) for support.

* t.p.billam@durham.ac.uk

- [1] L. Khaykovich *et al.*, *Science* **296**, 1290 (2002).
- [2] K. E. Strecker *et al.*, *Nature* **417**, 150 (2002).
- [3] S. L. Cornish, S. T. Thompson, and C. E. Wieman, *Phys. Rev. Lett.* **96**, 170401 (2006).
- [4] T. Dauxois and M. Peyrard, *Physics of Solitons* (Cambridge University Press, 2006).
- [5] V. Zakharov and A. Shabat, *Zh. Eksp. Teor. Fiz.* **61**, 118 (1971) [*Sov. Phys. JETP* **34**, 62 (1972)].
- [6] J. P. Gordon, *Opt. Lett.* **8**, 596 (1983).
- [7] J. Satsuma and N. Yajima, *Prog. Theor. Phys. Suppl.* **55**, 284 (1974).
- [8] Y. Kodama and A. Hasegawa, *Opt. Lett.* **16**, 208 (1991).
- [9] V. V. Afanasjev and V. A. Vysloukh, *J. Opt. Soc. Am. B* **11**, 2385 (1994).
- [10] A. D. Martin, C. S. Adams, and S. A. Gardiner, *Phys. Rev. Lett.* **98**, 020402 (2007); *Phys. Rev. A* **77**, 013620 (2008).
- [11] D. Poletti *et al.*, *Phys. Rev. Lett.* **101**, 150403 (2008).
- [12] N. G. Parker *et al.*, *J. Phys. B* **41**, 045303 (2008); *Physica D* **238**, 1456 (2009).
- [13] S. L. Cornish *et al.*, *Physica D* **238**, 1299 (2009).
- [14] E. A. Donley *et al.*, *Nature* **412**, 295 (2001); L. P. Pitaevskii, *Phys. Lett. A* **221**, 14 (1996).
- [15] N. G. Parker *et al.*, *J. Phys. B* **40**, 3127 (2007).
- [16] U. Al Khawaja *et al.*, *Phys. Rev. Lett.* **89**, 200404 (2002); K. E. Strecker *et al.*, *N. J. Phys.* **5**, 73 (2003).
- [17] L. D. Carr and J. Brand, *Phys. Rev. Lett.* **92**, 040401 (2004).
- [18] B. J. Dąbrowska-Wüster, S. Wüster, and M. J. Davis, *N. J. Phys.* **11**, 053017 (2009).
- [19] In this case, $\Psi(\mathbf{r}, t)$ factorizes into $\Psi(x, t)$ and the radial harmonic ground state, $\Psi(\mathbf{r}, t) = \Psi(x, t) \sqrt{m\omega_r/\pi\hbar} \exp[-m\omega_r(y^2 + z^2)/2\hbar]$, the latter of which can be integrated out [10].
- [20] Ensuring unit norm for $\psi(x, t)$ requires $\psi(x, t) = \sqrt{b_0}\Psi(x, t)$.
- [21] We consider an experiment using the hyperfine ground states $|F = 2, m_f = -2\rangle$ and $|3, -2\rangle$ of ^{85}Rb . We assume an instantaneous $\pi/2$ pulse on the two-photon rf/microwave transition coupling $|2, -2\rangle$ and $|3, -2\rangle$, and evolve the resulting state for time τ with magnetic field $\mathbf{B} = [B_0 + C(x - x_0)]\hat{\mathbf{B}}$. We assume the scattering length of the $|3, -2\rangle$ state and the inter-state scattering length is $a_{\infty} = -443a_0$ and model that of the $|2, -2\rangle$ state as $a_{\infty}[1 - \Delta/(B_0 + Cx - B_F)]$, where $\Delta = 10.7$ Gauss and $B_F = 155.0$ Gauss [22]. In soliton units, the components experience potentials $\Gamma \pm \gamma(x - x_0)$, where $\Gamma = |g_F||m_f|\mu_B(B_0 - B_F)/4m\omega_r^2|a_s|^2N^2$ and $\gamma = |g_F||m_f|\mu_B C\hbar/8m^2\omega_r^3|a_s|^3N^3$. After time τ we assume another instantaneous $\pi/2$ pulse and instantaneous expulsion of the $|3, -2\rangle$ component with resonant light. An approximation to Eq. (4) is obtained when, for example $\omega_x \approx 10 \times 2\pi$ Hz, $\omega_r \approx 150 \times 2\pi$ Hz, $N \approx 800$, $a_s \approx -20a_0$ ($B_0 \approx 166$ Gauss), $C \approx 75$ Gauss cm^{-1} and $\tau \approx 10\mu\text{s}$.
- [22] N. R. Claussen *et al.*, *Phys. Rev. A* **67**, 060701(R) (2003).
- [23] Note, for any amplitude A , that $A \text{sech}(Ax)$ is a stationary soliton solution to Eq. (1), with norm $2A$.
- [24] G. Boffetta and A. R. Osborne, *J. Comp. Phys.* **102**, 252 (1992).
- [25] Ensuring unit norm for $\psi(\mathbf{r}, t)$ requires $\psi(\mathbf{r}, t) = b_0^{3/2}\Psi(\mathbf{r}, t)$. Also, in the quasi-1D limit, the integrated axial density $\int_{-\infty}^{\infty} |\psi(\mathbf{r}, t)|^2 dy dz \rightarrow |\psi(x, t)|^2$.
- [26] In the case $k = 3$ quasi-1D behavior is reached (the phase dependence of C_{1D} ends) at $\lambda \approx 20$, but this has been omitted from the plotted range for clarity.
- [27] L. Khaykovich and B. A. Malomed, *Phys. Rev. A* **74**, 023607 (2006).